

When Theory Meets Experiment: What Does it Take to Accurately Predict ^1H NMR Dipolar Relaxation Rates in Neat Liquid Water from Theory?

Dietmar Paschek^{1, a)}, Johanna Busch¹, Angel Mary Chiramel Tony¹, Ralf Ludwig¹, Anne Strate¹, Nore Stolte², Harald Forbert³, and Dominik Marx²

¹⁾ *Institut für Chemie, Abteilung Physikalische und Theoretische Chemie, Universität Rostock, Albert-Einstein-Str. 27, D-18059 Rostock, Germany*

²⁾ *Lehrstuhl für Theoretische Chemie, Ruhr-Universität Bochum, D-44780 Bochum, Germany*

³⁾ *Center for Solvation Science ZEMOS, Ruhr-Universität Bochum, D-44780 Bochum, Germany*

(Dated: 2024/11/20 at 01:48:48)

In this contribution, we compute the ^1H nuclear magnetic resonance (NMR) relaxation rate of liquid water at ambient conditions. We are using structural and dynamical information from Coupled Cluster Molecular Dynamics (CCMD) trajectories generated at CCSD(T) electronic structure accuracy while considering also nuclear quantum effects in addition to consulting information from X-ray and neutron scattering experiments. Our analysis is based on a recently presented computational framework for determining the frequency-dependent NMR dipole-dipole relaxation rate of spin 1/2 nuclei from Molecular Dynamics (MD) simulations, which allows for an effective disentanglement of its structural and dynamical contributions, and is including a correction for finite-size effects inherent to MD simulations with periodic boundary conditions. A close to perfect agreement with experimental relaxation data is achieved if structural and dynamical informations from CCMD trajectories are considered including a re-balancing of the rotational and translational dynamics, according to the product of the self-diffusion coefficient and the reorientational correlation time of the H-H vector $D_0 \times \tau_{\text{HH}}$. The simulations show that this balance is significantly altered when nuclear quantum effects are taken into account. Our analysis suggests that the intermolecular and intramolecular contribution to the ^1H NMR relaxation rate of liquid water are almost similar in magnitude, unlike to what was predicted earlier from classical MD simulations.

Keywords: NMR, NMR Relaxation, Molecular Dynamics Simulations, Water, Diffusion

I. INTRODUCTION

The nuclear magnetic resonance (NMR) relaxation rate R_1 of ^1H nuclei in liquid water has been measured in 1966 by K. Krynicki¹ and shortly after that by E. v. Goldammer and M. D. Zeidler.² It was determined to be $R_1(\nu_{\text{H}}) = (0.280 \pm 0.003) \text{ s}^{-1}$ at a resonance frequency of $\nu_{\text{H}} = 28 \text{ MHz}$ at 298 K and ambient pressure conditions.¹ The question, we would like to answer in this contribution is: How well do we understand and can hence predict this relaxation rate purely based on theory almost 60 years later?

The primary mechanism for relaxation of spin 1/2 nuclei in NMR spectroscopy is due to the magnetic dipole-dipole interaction.^{3,4} Dipolar relaxation is sensitive to details of the intermolecular and intramolecular structure and can provide information about the molecular motions within a chemical system.⁵⁻⁷ Interpreting experimental data, however, often requires analytical models of the structure and dynamics to accurately describe the underlying time correlation functions.⁸⁻¹¹ Alternatively, also Molecular Dynamics (MD) simulations can be used to study NMR relaxation phenomena, thus circumventing the need for analytical models. This advantage has

been recognized early.^{12,13} More recently, *ab initio* MD (AIMD) simulations as well as simulations based on machine learning potentials have come into focus as they can go beyond the limitations of classical molecular model potentials¹⁴ and can even account for nuclear quantum effects.¹⁵ In addition, the electronic structure information from AIMD simulations also allows to determine quadrupolar NMR relaxation phenomena for nuclei with spin $> 1/2$.¹⁶⁻¹⁸

Dipolar NMR relaxation is due to the fluctuating fields resulting from the magnetic dipole-dipole interaction between two spins, which can be formally divided into intermolecular and intramolecular contributions. Here, the computation of intermolecular relaxation rates needs to take into account that diffusion coefficients obtained from MD simulations with periodic boundary conditions exhibit a non-negligible system size dependence.¹⁹⁻²² Moreover, the spectral densities at low frequencies cover motions extending over large distance ranges.²³ To deal with these problems, we have recently presented a computational framework to reliably determine the frequency-dependent intermolecular NMR dipole-dipole relaxation rate from MD simulations.^{24,25} Our approach is based on a separation of the intermolecular part into a purely diffusion-based component, which is described by the theory of Hwang and Freed⁹ and a “difference function” computed from MD simulations. It has been shown, that for long times this “difference function” quickly

^{a)} Electronic mail: dietmar.paschek@uni-rostock.de

decays to zero and can thus be computed from rather short MD simulation runs of modest size.^{24,25} The influence of system-size dependent diffusion coefficients can be dealt with by employing Yeh-Hummer^{19,20} corrected inter-diffusion coefficients for the Hwang and Freed model in combination with a Yeh-Hummer-inspired scaling of the “difference function”.^{24,25} By construction, this approach is capable of accurately predicting the correct low-frequency scaling behavior of the intermolecular NMR dipole-dipole relaxation rate.

We have recently computed the frequency-dependent intermolecular and intramolecular dipolar NMR relaxation rates of the ^1H nuclei in liquid water at 298 K based on simulations of the TIP4P/2005 model for water.^{24,25} Our calculations determine the relaxation rate to be $R_1(\nu_{\text{H}}) = 0.3164 \text{ s}^{-1}$ at a resonance frequency of $\nu_{\text{H}} = 28 \text{ MHz}$, which is 13% above the experimental value. In this contribution, we will show that this discrepancy has to be mostly attributed to the intramolecular relaxation rate $R_{1,\text{intra}}(\nu_{\text{H}})$ and is to a large part the consequence of a misrepresentation of the intramolecular H-H distance in the TIP4P/2005 model. To account for the influence of both the molecular structure and dynamics subject to nuclear quantum effects, we analyze Coupled Cluster Molecular Dynamics (CCMD) trajectories from path integral molecular dynamics simulations²⁶ based on a high-dimensional neural network potential (HDNNP)²⁷ that has been generated at CCSD(T) accuracy.^{15,28} In addition, we also consult structural information from neutron scattering experiments reported by Soper,²⁹ as well as a recent re-evaluation of intramolecular H-H distances based on a variety of experimental sources according to Faux et al.³⁰ We show that in addition to the intramolecular H-H distance a rebalancing of the reorientational dynamics of the H-H vector in liquid water to match the balance between reorientational and translational dynamics in CCMD simulations is essential for the agreement with experimental ^1H NMR relaxation rates.

II. THEORY

A. Dipolar NMR Relaxation and Correlations in the Structure and Dynamics of Molecular Liquids

The dipolar relaxation of NMR active nuclei in a liquid is determined by their magnetic dipolar interaction with all the nuclei in their surroundings and is subject to the time-dependent spatial correlations in the liquid. Here the NMR relaxation rate of nuclear spins with $I = 1/2$ is dominated by the dipole-dipole interaction.³ Hence the frequency-dependent relaxation rate is determined by the time dependence of the magnetic dipole-dipole coupling. For two like spins, it is described by^{3,12}

$$R_1(\omega) = \gamma^4 \hbar^2 I(I+1) \left(\frac{\mu_0}{4\pi} \right)^2 \{J(\omega) + 4J(2\omega)\}, \quad (1)$$

where $J(\omega)$ represents the spectral density of the time-dependent nuclear dipolar interaction and μ_0 specifies the permeability of free space. In case the of an isotropic fluid, the spectral density is given by¹²

$$J(\omega) = \frac{2}{5} \text{Re} \left\{ \int_0^\infty G(t) e^{i\omega t} dt \right\} \quad (2)$$

where $G(t)$ denotes the “dipole-dipole correlation function” which is available via^{12,31}

$$G(t) = \left\langle \sum_j r_{ij}^{-3}(0) r_{ij}^{-3}(t) P_2[\cos \theta_{ij}(t)] \right\rangle, \quad (3)$$

where $\cos \theta_{ij}(t)$ is the cosine of the angle between the connecting vectors \vec{r}_{ij} joining spins i and j at time 0 and at time t while $P_2[\dots]$ represents the second Legendre polynomial.¹²

By combining Equations 2 and 3, the spectral density

$$J(\omega) = \frac{2}{5} \left\langle \sum_j r_{ij}^{-6}(0) \right\rangle \text{Re} \left\{ \int_0^\infty G^n(t) e^{i\omega t} dt \right\} \quad (4)$$

can be expressed as being composed of a r_{ij}^{-6} averaged constant depending solely on the structure, and the Fourier-transform of a normalized correlation function $G^n(t) = G(t)/G(0)$, which is sensitive to the dynamical features of the liquid.

For the case of $\omega \rightarrow 0$ we obtain a relaxation rate

$$R_1(0) = \gamma^4 \hbar^2 I(I+1) \left(\frac{\mu_0}{4\pi} \right)^2 \cdot 2 \int_0^\infty G(t) dt, \quad (5)$$

where the integral over the dipole-dipole correlation function

$$\int_0^\infty G(t) dt = \left\langle \sum_j r_{ij}^{-6}(0) \right\rangle \tau_G \quad (6)$$

is the product of the r_{ij}^{-6} averaged constant and a correlation time τ_G , which is the time-integral of the normalized correlation function

$$\tau_G = \int_0^\infty G^n(t) dt, \quad (7)$$

characterizing the dynamical processes within the liquid.

For convenience, one may divide the spins j into different classes according to whether they belong to the same molecule as spin i , or not, thus arriving at an inter- and intramolecular contribution to the relaxation rate

$$R_1(\omega) = R_{1,\text{inter}}(\omega) + R_{1,\text{intra}}(\omega), \quad (8)$$

which are related to corresponding intermolecular and intramolecular dipole-dipole correlation functions $G_{\text{intra}}(t)$

and $G_{\text{inter}}(t)$. The intramolecular contribution is due to molecular reorientations and conformational changes, while the intermolecular contributions are largely affected by the translational mobility (i.e. diffusion), but is also sensitive to local mutual reorientations, librational motions, and conformational changes of adjacent molecules.

a. Intermolecular Contributions: The structure of a liquid can be described by the intermolecular site-site pair correlation functions $g_{ij}(r)$, denoting the probability of finding a second atom of type j in a distance r from a reference site of type i according to³²

$$g_{ij}(r) = \frac{1}{N_i \rho_j} \left\langle \sum_{k=1}^{N_i} \sum_{l=1}^{N_j} \delta(\vec{r} - \vec{r}_{kl}) \right\rangle, \quad (9)$$

where ρ_j is the number density of atoms (or spins) of type j . The pre-factor of the intermolecular dipole-dipole correlation function is hence related to the pair distribution function via an r^{-6} -weighted integral over the pair correlation function

$$\left\langle \sum_j r_{ij}^{-6}(0) \right\rangle = \rho_j 4\pi \int_0^\infty r^{-6} g_{ij}(r) r^2 dr. \quad (10)$$

The integral in Equation 10 contains all the structural correlations affecting the spin pairs under consideration. Averaged intermolecular distances between two spins α and β are thus represented by the integral

$$I_{\alpha\beta} = 4\pi \int_0^\infty r^{-6} g_{\alpha\beta}(r) r^2 dr. \quad (11)$$

Relating the structure of the liquid to a structureless hard-sphere fluid, the integral $I_{\alpha\beta}$ can be also described by a ‘‘distance of closest approach’’ (DCA) $d_{\alpha\beta}$, which represents an integral of the same size, but over a step-like unstructured pair correlation function according to

$$I_{\alpha\beta} = 4\pi \int_{d_{\alpha\beta}}^\infty r^{-6} \cdot 1 \cdot r^2 dr = \frac{4\pi}{3} \cdot \frac{1}{d_{\alpha\beta}^3}. \quad (12)$$

Hence the DCA can be determined with the knowledge of $I_{\alpha\beta}$ as

$$d_{\alpha\beta} = \left[\frac{4\pi}{3} \cdot \frac{1}{I_{\alpha\beta}} \right]^{1/3}. \quad (13)$$

This DCA is conceptually identical to the distance used in the structureless hard-sphere diffusion model as outlined by Freed and Hwang.⁹

To determine the $d_{\alpha\beta}$ in this paper, the integral $I_{\alpha\beta}$ is evaluated via

$$I_{\alpha\beta} \approx 4\pi \int_0^{R_c} r^{-6} g_{\alpha\beta}(r) r^2 dr + \frac{4\pi}{3} R_c^{-3} \quad (14)$$

by numerically integrating over the pair correlation function up to a cutoff distance R_c and then corrected by adding the term $4\pi/(3R_c^3)$ as long-range correction.

b. Intramolecular Contribution: Intramolecular correlations are computed directly by summation over all involved spin pairs. For the case of water, there remains only a single intramolecular dipole-dipole interaction. By definition does a rigid water model such as TIP4P/2005 possess only a fixed H-H distance. Therefore the intramolecular contribution to the relaxation rate is dominantly based on the reorientational correlation function of the intramolecular H-H vector

$$C_2^{\text{HH}}(t) = \langle P_2[\vec{u}_{\text{HH}}(0) \cdot \vec{u}_{\text{HH}}(t)] \rangle, \quad (15)$$

where \vec{u}_{HH} is a unit vector oriented along the intramolecular H-H axis and $P_2[\dots]$ indicates the second Legendre polynomial.

B. Intermolecular Dipole-Dipole Relaxation: MD-Simulation and the Theory of Hwang and Freed

We define the normalized intermolecular dipole-dipole correlation function as

$$G_{\text{inter}}^{\text{n}}(t) = G_{\text{inter}}(t)/G_{\text{inter}}(0). \quad (16)$$

Following the approach of Hwang and Freed⁹, we can give an analytical expression for the dipole-dipole correlation function of two diffusing particles with a DCA d , reflecting boundary conditions at $r = d$, and an inter-diffusion coefficient D' using

$$G_{\text{inter}}^{\text{n,HF}}(u) = \frac{54}{\pi} \int_0^\infty \frac{x^2 \cdot e^{-u \cdot x^2} dx}{81 + 9x^2 - 2x^4 + x^6}, \quad (17)$$

where u denotes a reduced timescale

$$u \equiv \frac{D't}{d^2}, \quad (18)$$

and x represents a reduced inverse distance scale $x \equiv d/r$. For long times, ultimately, $G_{\text{inter}}^{\text{n,HF}}(t)$ exhibits a $t^{-3/2}$ scaling behavior and can be expressed using the reduced time-scale u as⁹

$$\lim_{u \rightarrow \infty} G_{\text{inter}}^{\text{n,HF}}(u) \approx \frac{1}{6\sqrt{\pi} \cdot u^{3/2}}. \quad (19)$$

The correct representation of the power-law behavior at long times is particularly important for properly describing the low-frequency limit of the corresponding spectral density function $\lim_{\omega \rightarrow 0} J_{\text{inter}}^{\text{HF}}(\omega) \propto \sqrt{\omega}$. Using the normalized dipole-dipole correlation function of the Hwang and Freed theory according to Equation 17, the corresponding intermolecular spectral density is given by

$$J_{\text{inter}}^{\text{HF}}(\omega_u) = \frac{2}{5} \left\langle \sum_j r_{ij}^{-6}(0) \right\rangle \cdot J_{\text{inter}}^{\text{n,HF}}(\omega_u), \quad (20)$$

where $J_{\text{inter}}^{\text{n,HF}}(\omega_u)$ represents the “normalized” Hwang-Freed spectral density, obtained as a Fourier transformation of $G_{\text{inter}}^{\text{n}}(t)$ with

$$J_{\text{inter}}^{\text{n,HF}}(\omega_u) = \frac{54}{\pi} \cdot \frac{d^2}{D'} \times \int_0^\infty \frac{dx}{(81 + 9x^2 - 2x^4 + x^6)(1 + \omega_u^2/x^4)}, \quad (21)$$

where $\omega_u \equiv \omega \cdot d^2/D'$ denotes a reduced frequency scale, corresponding to the reduced time scale u . From Equation 21 follows directly the spectral density for $\omega_u \rightarrow 0$

$$J_{\text{inter}}^{\text{HF}}(0) = \frac{2}{5} \left\langle \sum_j r_{ij}^{-6}(0) \right\rangle \cdot \frac{4}{9} \cdot \frac{d^2}{D'}, \quad (22)$$

where

$$\tau_{\text{G,HF}} = J_{\text{inter}}^{\text{n,HF}}(0) = \frac{4}{9} \cdot \frac{d^2}{D'} \quad (23)$$

represents the intermolecular dipole-dipole “correlation-time” obtained as integral over the normalized dipole-dipole correlation function $G_{\text{inter}}^{\text{n,HF}}(t)$.

The Hwang and Freed theory outlined above describes the behavior of random walkers sampled from an infinitely large system. In computer simulations of condensed matter systems, however, we mostly deal with finite system sizes using periodic boundary conditions, thus limiting the volume from which the starting positions are sampled. We have recently shown that the problem can be hedged by approximating the effect caused by the limited sampling volumes on the correlation function according to the Hwang and Freed model given in Equation 17, by employing a nonzero lower boundary value $x_{\text{P}} = \theta \cdot d/R$ with $\theta \approx 2.53$ for the integral of Equation 17, leading to

$$G_{\text{inter}}^{\text{n,HF}}(u, x_{\text{P}}) = \frac{1}{A(x_{\text{P}})} \int_{x_{\text{P}}}^\infty \frac{x^2 \cdot e^{-u \cdot x^2} dx}{81 + 9x^2 - 2x^4 + x^6}, \quad (24)$$

recognizing that the variable x is essentially representing an inverse distance. The parameter θ has been determined empirically to provide the best agreement with data obtained random walker simulations for various values of R/d .^{24,25} Here the normalisation constant

$$A(x_{\text{P}}) = \int_{x_{\text{P}}}^\infty \frac{x^2 dx}{81 + 9x^2 - 2x^4 + x^6} \quad (25)$$

needs to be computed by numerical integration, except for $A(x_{\text{P}}=0) = \pi/54$. The deviation of the approximate expression given by Equation 24 from Equation 17 can then be quantified by

$$s(u, x_{\text{P}}) = \frac{G_{\text{inter}}^{\text{n,HF}}(u, x_{\text{P}}=0)}{G_{\text{inter}}^{\text{n,HF}}(u, x_{\text{P}})}, \quad (26)$$

where the numerator represents Equation 17. As shown in Ref.^{24,25}, Equation 26 very well captures the initial effect due to the limited sampling volumes over a broad range of R/d values that would correspond to liquid water simulations ranging from 2000 to about 16000 water molecules in a cubic unit cell. Since for longer times Equation 17 leads to an overcorrection, we have introduced a time-limit t_{tr} , characterizing up to which the correction could be meaningfully applied. Realising that the corresponding timescale is governed by the ratio of the radius R (or the half box size $L/2$) and the inter-diffusion coefficient D' , we get

$$t_{\text{tr}} = \frac{R^2}{4\pi D'} = \frac{L^2}{16\pi D'}, \quad (27)$$

which will consistently result in a time range where the scaling function $s(u, x_{\text{P}}) \leq 1.25$.

III. METHODS

We have performed classical MD simulations of liquid water using the TIP4P/2005 model³³, which has been demonstrated to accurately describe the properties of water compared to other simple rigid nonpolarizable water models.³⁴ All simulations were carried out at 298 K under NVT conditions using system sizes of 512, 1024, 2048, 4096, and 8192 molecules. After sufficient equilibration, MD simulations of 1 ns length each were performed using GROMACS 5.0.6.^{35,36} The integration time step for all simulations was 2 fs. The temperature of the simulated systems was controlled by employing the Nosé-Hoover thermostat.^{37,38} More details about the simulations are given in Ref.^{24,25}.

To go beyond the accuracy of the TIP4P/2005 force field and understand the effect of quantum delocalization of nuclei, we analyzed constant-volume ring polymer molecular dynamics (RPMD) simulations³⁹ with 32 Trotter replica (“beads”) of H₂O and D₂O at 298 K with their experimental densities at 1 atm^{40,41}, and computed structural properties, diffusion coefficients, $C_2(t)$ orientational correlation functions, and τ_2 orientational correlation times. The inclusion of nuclear quantum degrees of freedom has recently been demonstrated to be essential for reproducing the structural and dynamical properties of liquid water based on very accurate interactions.^{15,42,43} The RPMD simulations were performed with the Coupled Cluster Molecular Dynamics (CCMD) approach for liquid water¹⁵, which employs a high-dimensional neural network potential (HDNNP)^{27,44} to simulate liquid water with CCSD(T) accuracy. The analyzed trajectories were produced with CP2K^{45,46} with its path integral⁴⁷ and HDNNP⁴⁸ modules. Individual RPMD trajectories were 100 ps long with a 0.25 fs time step and were initialized from configurations drawn at 10 ps intervals from path integral molecular dynamics simulations thermostatted with the path integral Langevin equation approach.⁴⁹

Structural properties, reorientational correlation functions $C_2(t)$, and correlation times τ_2 were obtained from RPMD trajectories with 256 molecules, with a total length of 5 and 11 ns for D₂O and H₂O, respectively. Structural properties were extracted based on bead positions printed at 100 fs intervals. $C_2(t)$ functions were obtained using bead positions⁵⁰ at 1 fs intervals, and we computed τ_2 of the intramolecular H–H and D–D vectors, τ_2^{HH} and τ_2^{DD} , by integrating $C_2^{\text{HH}}(t)$ and $C_2^{\text{DD}}(t)$ from the RPMD simulations from 0 to 40 ps following earlier work⁵¹, with error bars as described previously¹⁵. Self-diffusion coefficients were computed from individual simulations via a maximum entropy formalism⁵² based on molecular centroid positions at 2 fs intervals, and system-size independent self-diffusion coefficients D_0 were obtained by extrapolating results from cubic simulation cells containing 64, 96, 128 and 256 molecules to the infinite box size.^{19,53} In total, we analyzed 5 and 11 ns of RPMD simulations at each box size for D₂O and H₂O, respectively.

Inter- and intramolecular dipole-dipole correlation functions obtained from classical MD simulation data were computed using our open-source software package “MDorado” which is available via GitHub (github.com/Paschek-Lab/MDorado). Our open source software “FreeDRelax” for performing finite-size cutoff-corrections to the intermolecular dipole-dipole correlation functions and for computing the inter- and intramolecular spectral densities and relaxation rates discussed in section II is also available via GitHub (github.com/Paschek-Lab/FreeDRelax).

IV. RESULTS AND DISCUSSION

A. Transport Properties

Classical MD simulations of TIP4P/2005 water at 298 K were carried out at a density of 0.99712 g cm⁻³ corresponding to a pressure of 1 bar for system sizes between 512 and 8192 molecules. Data characterizing the simulations can be found in TABLE 1 of Ref.^{24,25}. The system-size independent self-diffusion coefficient and viscosity of the TIP4P/2005 model have been recently re-evaluated by us for the same conditions as used here based on the “OrthoBoXY” approach⁵⁴ leading to a diffusion coefficient of $D_0 = (2.299 \pm 0.005) \times 10^{-9} \text{ m}^2 \text{ s}^{-1}$ and a viscosity of $\eta = (0.860 \pm 0.018) \text{ mPa} \cdot \text{s}$.⁵⁴ These data are perfectly consistent with the simulations of Gonzales and Abascal who report a viscosity value of 0.855 mPa · s for TIP4P/2005⁵⁵, and agree with the experimental self-diffusion coefficient at 298 K of $2.3 \times 10^{-9} \text{ m}^2 \text{ s}^{-1}$ by Krynicki⁵⁶ and $2.299 \times 10^{-9} \text{ m}^2 \text{ s}^{-1}$ by Holz and co-workers using ¹H PFG NMR experiments.⁵⁷ The system-size independent self-diffusion coefficients D_0 based on CCMD simulations²⁸ for H₂O with $(2.34 \pm 0.09) \times 10^{-9} \text{ m}^2 \text{ s}^{-1}$ and for D₂O with $(1.86 \pm 0.02) \times 10^{-9} \text{ m}^2 \text{ s}^{-1}$ are also consistent with the experimental data given by

Mills for H₂O and D₂O with $2.299 \times 10^{-9} \text{ m}^2 \text{ s}^{-1}$, and $1.872 \times 10^{-9} \text{ m}^2 \text{ s}^{-1}$ respectively.⁵⁸ The agreement of the CCMD simulations with both H₂O and D₂O experimental self-diffusion coefficients is suggesting that the chosen ring polymer molecular dynamics (RPMD) simulation setup discussed in Ref.¹⁵ is perfectly capable of capturing the effect of quantum delocalization of nuclei on the dynamical properties of liquid water.^{15,28}

B. Intramolecular Relaxation

To describe the long-time intramolecular dipole-dipole correlation functions we do not employ a physics-based mechanistic model, but the empirical Kohlrausch-Williams Watts (KWW) function using

$$G_{\text{intra}}^{\text{n,K}}(t) = A_{\text{K}} \cdot \exp \left[- \left(\frac{t}{\tau_{\text{K}}} \right)^{\beta_{\text{K}}} \right]. \quad (28)$$

This empirical model has been fitted to the computed $G_{\text{intra}}^{\text{n,MD}}(t)$ over a time interval between 1 ps and 100 ps. Here, the KWW function can be regarded as representing a distribution of relaxation times, where the parameter β describes the width of this distribution. Note, that it is common practice to assume a distribution of relaxation times to describe the intramolecular contribution to the NMR relaxation in molecular liquids.⁵⁹ This phenomenon has been recently extensively analyzed by Asthagiri and co-workers.^{60,61}

In FIG. 1 both functions are plotted from data of the CCMD simulations of H₂O. A log-linear representation of the data, including the difference function

$$\Delta G_{\text{intra}}^{\text{n}}(t) = G_{\text{intra}}^{\text{n,MD}}(t) - G_{\text{intra}}^{\text{n,K}}(t) \quad (29)$$

is shown in FIG. 1. Significant differences between $G_{\text{intra}}^{\text{n,MD}}(t)$ and $G_{\text{intra}}^{\text{n,K}}(t)$ are restricted to a time-interval $t \leq 1$ ps. Hence the intramolecular correlation time τ_{G} was computed as an integral over $G_{\text{intra}}^{\text{n,MD}}(t)$, which can be splitted into two terms according to

$$\tau_{\text{G}} = \tau_{\text{G,K}} + \Delta\tau_{\text{G}} \quad (30)$$

with

$$\tau_{\text{G,K}} = A_{\text{K}} \tau_{\text{K}} \beta_{\text{K}}^{-1} \Gamma(\beta_{\text{K}}^{-1}), \quad (31)$$

where $\Gamma(\dots)$ represents the Gamma-function.

To compute the intramolecular spectral density from MD simulation, we use

$$J_{\text{intra}}^{\text{n,MD}}(\omega) = J_{\text{intra}}^{\text{n,K}}(\omega) + \Delta J_{\text{intra}}^{\text{n}}(\omega) \quad (32)$$

with

$$\Delta J_{\text{intra}}^{\text{n}}(\omega) \approx \int_0^{t^*} \Delta G_{\text{intra}}^{\text{n}}(t) \cos(\omega t) dt. \quad (33)$$

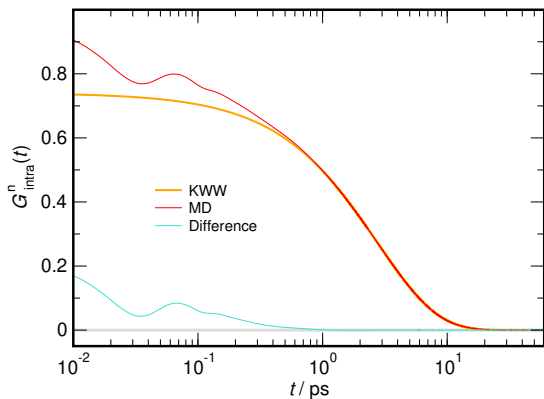


FIG. 1. Normalized intramolecular dipole-dipole correlation function $G_{\text{intra}}^n(t)$ computed for water at 298 K. Intramolecular dynamics from CCMD simulations of H_2O at CCSD(T) accuracy which include nuclear quantum effects. Solid red line: $G_{\text{intra}}^{\text{n,MD}}(t)$. Solid orange line: $G_{\text{intra}}^{\text{n,K}}(t)$ according to Equation 28 using $A_K = 0.73995$, $\tau_K = 2.7622$ ps, and $\beta_K = 0.9057$, and $\Delta G_{\text{intra}}^n(t) = G_{\text{intra}}^{\text{n,MD}}(t) - G_{\text{intra}}^{\text{n,K}}(t)$.

Here the computation of the integral in Equation 33 is as well performed numerically, employing the trapezoidal rule up to a time $t^* = 5$ ps, where both functions $G_{\text{intra}}^{\text{n,MD}}(t)$ and $G_{\text{intra}}^{\text{n,K}}(t)$ become effectively indistinguishable. The Fourier-transform of $G_{\text{intra}}^{\text{n,K}}(t)$, defined in Equation 28, $J_{\text{intra}}^{\text{n,K}}(\omega)$, needs, however, to be computed numerically, due to the lack of an analytical Fourier-transform equivalent of the KWW function. To compute $J_{\text{intra}}^{\text{n,K}}(\omega)$ properly, we have tested the convergence of the numerical cosine-transform evaluation by comparing it to the limiting value for $\omega \rightarrow 0$. The intramolecular ^1H NMR relaxation rate following Equation 1 is finally computed via

$$R_{1,\text{intra}}(\omega) = \gamma_{\text{H}}^4 \hbar^2 \cdot \frac{3}{4} \cdot \left(\frac{\mu_0}{4\pi}\right)^2 \cdot \frac{2}{5} \cdot \frac{1}{r_{\text{HH}}^6} \times \quad (34)$$

$$\left\{ J_{\text{intra}}^{\text{n,MD}}(\omega) + 4 J_{\text{intra}}^{\text{n,MD}}(2\omega) \right\},$$

where r_{HH} represents the properly weighted intramolecular H-H distance.

As discussed in section II, the normalized intramolecular dipole-dipole correlation function $G_{\text{intra}}^{\text{n,MD}}(t)$ is dominated by the reorientational correlation function $C_2^{\text{HH}}(t)$ of the intramolecular H-H vector as defined by Equation 15. For the case of the rigid TIP4P/2005 model, $G_{\text{intra}}^{\text{n,MD}}(t)$ is perfectly identical with $C_2^{\text{HH}}(t)$, since the distance of the H-H vector is being kept fixed during the simulation. This is, however, not the case for the CCMD simulations, where no constraints with respect to bond distances and bond angles exist. Here the length of the H-H connecting vector will be mostly affected by intramolecular bond bending vibrational motions. Bond bending and reorientational motions are, however, well de-correlated since the H-H vibrations are about two orders of magnitude faster than the reorientational mo-

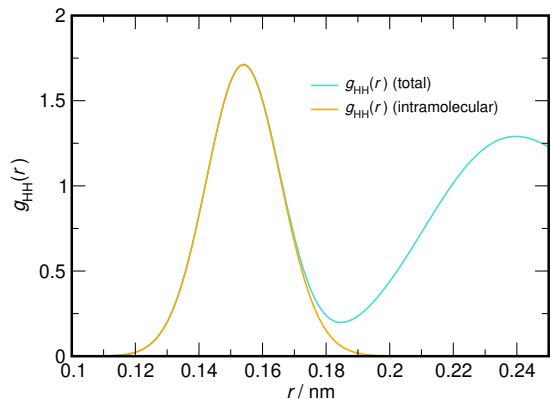


FIG. 2. Intramolecular and total H-H radial distribution function $g_{\text{HH}}(r)$ for $T = 298$ K as obtained from CCMD simulations of H_2O . The average intramolecular H-H distance is obtained to be $\langle r_{\text{HH}}^{-3} \rangle^{-1/3} = 154.1$ pm.

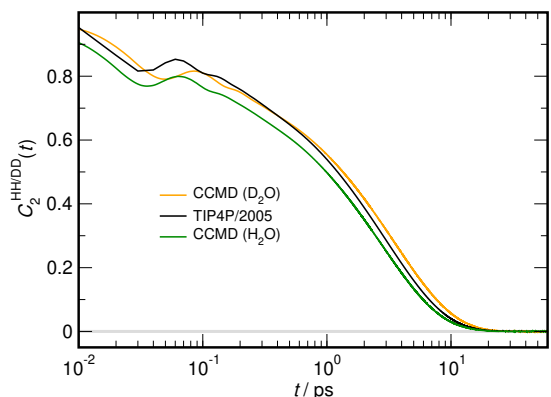


FIG. 3. Reorientational correlation function of the H-H vector $C_2^{\text{HH}}(t)$. The corresponding reorientational correlation times are: $\tau_2^{\text{HH}} = (2.16 \pm 0.02)$ ps (CCMD H_2O), $\tau_2^{\text{HH}} = (2.48 \pm 0.01)$ ps (TIP4P/2005), and $\tau_2^{\text{DD}} = (2.80 \pm 0.04)$ ps (CCMD D_2O).

tions, such that

$$G_{\text{intra}}^{\text{n,MD}}(t) \approx \frac{\langle r_{\text{HH}}^{-3}(0)r_{\text{HH}}^{-3}(t) \rangle}{\langle r_{\text{HH}}^{-6} \rangle} \cdot C_2^{\text{HH}}(t). \quad (35)$$

A consequence of the fast de-correlation of the oscillatory motion is that the distance-dependent time correlation function is nearly instantly quenched, which leads to

$$G_{\text{intra}}^{\text{n,MD}}(t) \approx \frac{\langle r_{\text{HH}}^{-3} \rangle^2}{\langle r_{\text{HH}}^{-6} \rangle} \cdot C_2^{\text{HH}}(t). \quad (36)$$

This would correspond to employing $C_2^{\text{HH}}(t)$ instead of $G_{\text{intra}}^{\text{n,MD}}(t)$ to determine $J_{\text{intra}}^{\text{n,MD}}(\omega)$ in Equation 34 while using for the term $1/r_{\text{HH}}^6$ in Equation 34

$$\frac{1}{r_{\text{HH}}^6} = \langle r_{\text{HH}}^{-3} \rangle^2. \quad (37)$$

In Refs. 24,25 we have employed the intramolecular H-H distance of the TIP4P/2005 model with $r_{\text{HH}} =$

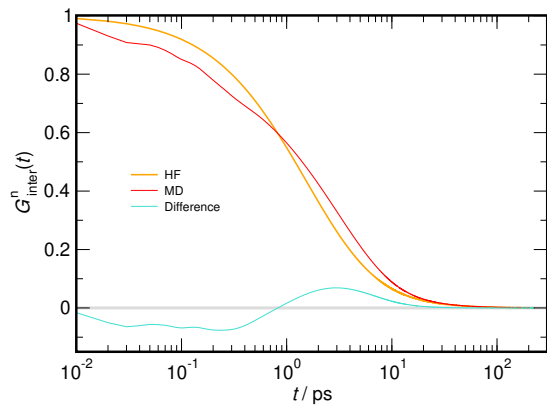


FIG. 4. Normalized intermolecular dipole-dipole correlation function $G_{\text{inter}}^n(t)$ computed for water at 298 K. Intermolecular dynamics from classical MD simulations of TIP4P/2005 water. Solid red line: $G_{\text{inter}}^{\text{n,MD}}(t)$. Solid orange line: $G_{\text{inter}}^{\text{n,HF}}(t)$ computed using data shown in TABLE I of Ref. ^{24,25}. Solid turquoise line: difference function $\Delta G_{\text{inter}}^n(t) = G_{\text{inter}}^{\text{n,MD}}(t) - G_{\text{inter}}^{\text{n,HF}}(t)$.

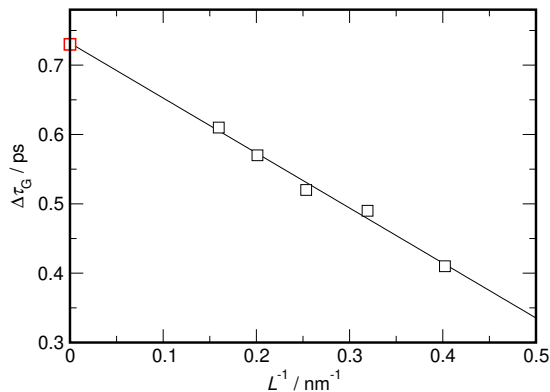


FIG. 5. Scaling of the computed intermolecular $\Delta\tau_G$ for TIP4P/2005 water at 298 K given in TABLE I of Ref. ^{24,25} as a function of the inverse box length L^{-1} , analogous to the scaling of the translational diffusion coefficient suggested by Yeh and Hummer.¹⁹ The extrapolated value for $L \rightarrow \infty$ is indicated in red.

151.4 pm leading to an intramolecular relaxation rate of $R_{1,\text{intra}}(\nu_{\text{H}}) = 0.1759 \text{ s}^{-1}$, which is practically frequency independent for resonance frequencies $\nu_{\text{H}} \leq 400 \text{ MHz}$. In 2021 Faux et al.³⁰ revisited the reorientational dynamics of water and argued in favour of using the Lévy rotor model as the most appropriate description. They also collected information about the intramolecular H-H distances from a variety of experimental sources and concluded a distance of $\langle r_{\text{HH}}^{-3} \rangle^{-1/3} = (154.5 \pm 0.7) \text{ pm}$ as a consensus distance for liquid water in the condensed phase (see supporting information of Ref.³⁰). This larger distance would by itself lead to a reduction of the intramolecular relaxation rate by about 11.45% compared to the value given above.^{24,25} Here, we have computed the average intramolecular H-H distance according to Equa-

tion 37 from the intramolecular pair correlation function obtained from our CCMD simulations of H₂O shown in FIG. 2, yielding a value of $\langle r_{\text{HH}}^{-3} \rangle^{-1/3} = 154.1 \text{ pm}$, which is in excellent agreement with the estimate of Faux et al.

In FIG. 3 we show $C_2^{\text{HH}}(t)$ reorientational correlation functions obtained for H₂O and D₂O obtained from our CCMD simulations in addition to the reorientational correlation function obtained from the purely classical TIP4P/2005 simulations. We would like to emphasize that there is a great similarity between the librational short-time features of the TIP4P/2005 model and the CCMD data for H₂O. The CCMD derived function for H₂O is, however, situated significantly below the classical TIP4P/2005 data, suggesting that the correlation function is quenched due to the quantum delocalization of the hydrogen nuclei. This is supported by the CCMD data for D₂O also shown in FIG. 3, where this quenching effect is less pronounced. For D₂O, the larger reduced mass also leads to a visibly enlarged librational frequency as indicated by its increased oscillation period. The corresponding reorientational correlation time for H₂O with $\tau_2^{\text{HH}} = (2.162 \pm 0.017) \text{ ps}$, is accordingly reduced by about 12.8% compared to the $\tau_2^{\text{HH}} = (2.48 \pm 0.01) \text{ ps}$ of the TIP4P/2005 model, while the value for D₂O with $\tau_2^{\text{DD}} = (2.80 \pm 0.04) \text{ ps}$ is larger than both. By using $\tau_2^{\text{HH}} \approx \tau_{\text{G}}$ and $r_{\text{HH}} = 154.1 \text{ pm}$ according to Equation 34, we compute an intramolecular relaxation rate of $\lim_{\omega \rightarrow 0} R_{1,\text{intra}}(\omega) = 0.1380 \text{ s}^{-1}$ in the extreme narrowing limit for H₂O from CCMD simulations, which is 21.6% smaller than the value obtained for the TIP4P/2005 model.

The various dynamical modes within a liquid are intricately related to the overall fluidity of the liquid matrix. According to hydrodynamic theory the translational and rotational dynamics are related to the viscosity of the fluid via the Stokes-Einstein (SE) and Stokes-Einstein-Debye (SED) relations, respectively. Combining both SE and SED relations lead to the expression⁶²

$$D_0 \times \tau_l = \frac{4}{3} \cdot \frac{1}{l(l+1)} \cdot R_{\text{h}}^2, \quad (38)$$

where D_0 is the translational self-diffusion coefficient, τ_l is the reorientational correlation time determined from a correlation function of a l -th order Legendre-polynomial, while R_{h} represents the hydrodynamic radius. The observation that the corresponding expression $\tau_l/\tau_l' = l'(l'+1)/(l(l+1))$ is not fulfilled for certain molecular systems has been regarded as an indication of a “break-down” of the Debye model.^{63,64} Moreover, given the important role that hydrogen bond exchange plays in the detailed mechanism of both water reorientation^{65,66} and water diffusion⁶⁷, it might even seem surprising how well the computed hydrodynamic radius agrees with the actual diameter of a water molecule⁶⁸ (at least for water under ambient conditions). In essence, however, Equation 38 describes a balance between reorientational and translational dynamics that is often surprisingly close to what has been predicted according to the hydrodynamic

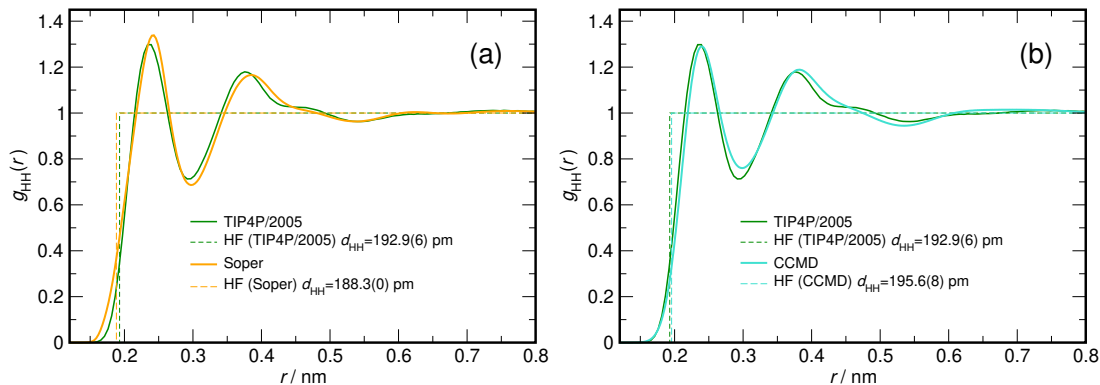


FIG. 6. Intermolecular H-H radial distribution function $g_{\text{HH}}(r)$ for $T=298$ K in addition to the corresponding step-like $g_{\text{HH}}(r)$ according to the Hwang and Freed theory with DCAs of d_{HH} as indicated. a) A comparison of the radial distribution functions obtained for the TIP4P/2005 model^{24,25} and from neutron scattering data according to Soper.²⁹ b) A comparison of the radial distribution functions obtained for the TIP4P/2005 model^{24,25} and from CCMD simulations of H₂O.

theory.⁶³ Note that delocalization of the H nuclei might affect translational and reorientational modes in liquid water differently and will thus have an effect on this balance. To investigate this effect quantitatively, we have computed the term $D_0 \times \tau_2^{\text{HH}}$ for all three systems under consideration. Here we notice a systematic variation with $D_0 \times \tau_2^{\text{HH}} = 0.506 \text{ \AA}^2$ for H₂O from CCMD simulations, $D_0 \times \tau_2^{\text{DD}} = 0.521 \text{ \AA}^2$ for D₂O from CCMD simulations, and $D_0 \times \tau_2^{\text{HH}} = 0.570 \text{ \AA}^2$ for the classical TIP4P/2005 simulations. It is important to realize that the inclusion of nuclear quantum delocalization in the simulation affects the reorientational dynamics of water more strongly than the translational motion, leading to a decrease of $D_0 \times \tau_2^{\text{HH}}$ for H₂O as compared to D₂O. Moreover, both values are significantly smaller than $D_0 \times \tau_2^{\text{HH}} = 0.570 \text{ \AA}^2$ computed here for the purely classical simulation of TIP4P/2005 water. We would like to point out that, in addition to the intramolecular H-H distance, a correct representation of this $D_0 \times \tau_2^{\text{HH}}$ balance is essential for providing an accurate estimate for the intramolecular relaxation rate $R_{1,\text{intra}}$. The diffusion coefficient for H₂O from CCMD simulations is found to be slightly larger than the experimental self-diffusion coefficient. To account for the effect on this balance, we suggest the following procedure for determining τ_G

$$\tau_G \approx \tau_2^{\text{HH}} \times \frac{D_0(\text{CCMD, H}_2\text{O})}{D_0(\text{expt.})}. \quad (39)$$

When including this small modification, we compute as the best estimate for the intramolecular relaxation rate according to Equation 34 of $\lim_{\omega \rightarrow 0} R_{1,\text{intra}}(\omega) = 0.1404 \text{ s}^{-1}$ in the extreme narrowing limit for H₂O. Computed values for various frequencies ν_{H} using the spectral density function $J_{\text{intra}}^{\text{n,MD}}(\omega)$ obtained from CCMD simulations can be found in TABLE I.

C. Intermolecular Relaxation

For long times $G_{\text{inter}}^{\text{n}}(t)$ shows a $t^{-3/2}$ scaling behavior and the curve determined from MD simulation asymptotically approaches that of the Hwang and Freed model. In Ref.^{24,25} we have shown that for times $t \geq t_{\text{tr}}$ both curves are practically indistinguishable. A log-linear representation of the data, including the difference function

$$\Delta G_{\text{inter}}^{\text{n}}(t) = G_{\text{inter}}^{\text{n,MD}}(t) - G_{\text{inter}}^{\text{n,HF}}(t) \quad (40)$$

is shown in FIG. 4. Note that the difference function is negative up to a time of about 1 ps, then turns positive until it asymptotically approaches zero. These negative and positive contributions are due to a deviation of the dynamics of the ¹H nuclei in liquid water from a continuous micro-step diffusion mechanism assumed in the Hwang-Freed model. They are due to both, the librational motions of the water molecules, and the jump-like reorientational dynamics of water molecules discussed in detail by D. Laage and J.T. Hynes.^{65,66} The intermolecular correlation time τ_G can be computed as an integral over $G_{\text{inter}}^{\text{n,MD}}(t)$, which can hence be splitted into two terms according to

$$\tau_G = \tau_{G,\text{HF}} + \Delta\tau_G \quad (41)$$

with $\tau_{G,\text{HF}} = 4/9 \cdot d_{\text{HH}}^2/D'$ following Equation 23. Here $\Delta\tau_G$ can be computed comfortably via numerical integration of

$$\Delta\tau_G \approx \int_0^{t_{\text{tr}}} \Delta G_{\text{inter}}^{\text{n}}(t) dt \quad (42)$$

due to the short-time nature of $\Delta G_{\text{inter}}^{\text{n}}(t)$. To compute the intermolecular spectral density from MD simulation, we use

$$J_{\text{inter}}^{\text{n,MD}}(\omega) = J_{\text{inter}}^{\text{n,HF}}(\omega) + \Delta J_{\text{inter}}^{\text{n}}(\omega) \quad (43)$$

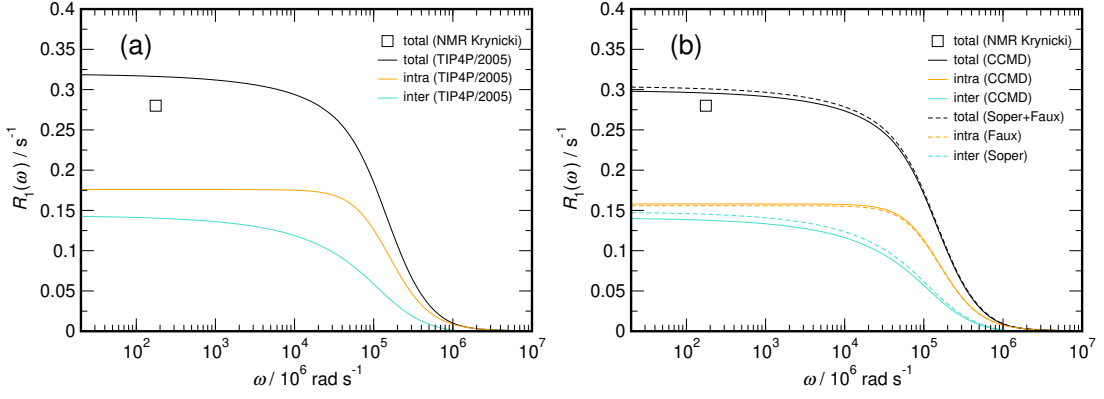


FIG. 7. Frequency-dependent ^1H NMR relaxation rate $R_1(\omega)$ of water at 298 K at a density of 0.997 g cm^{-3} a) based on TIP4P/2005 model data as in Ref.^{24,25} using $D' = 2D_0$ with $D_0 = 2.30 \times 10^{-9} \text{ m}^2 \text{ s}^{-1}$ and b) employing refined structural parameters for d_{HH} and $\langle r_{\text{HH}}^{-3} \rangle^{-1/3}$ either based on CCMD simulations or the experimental data of Soper²⁹ and Faux et al.³⁰.

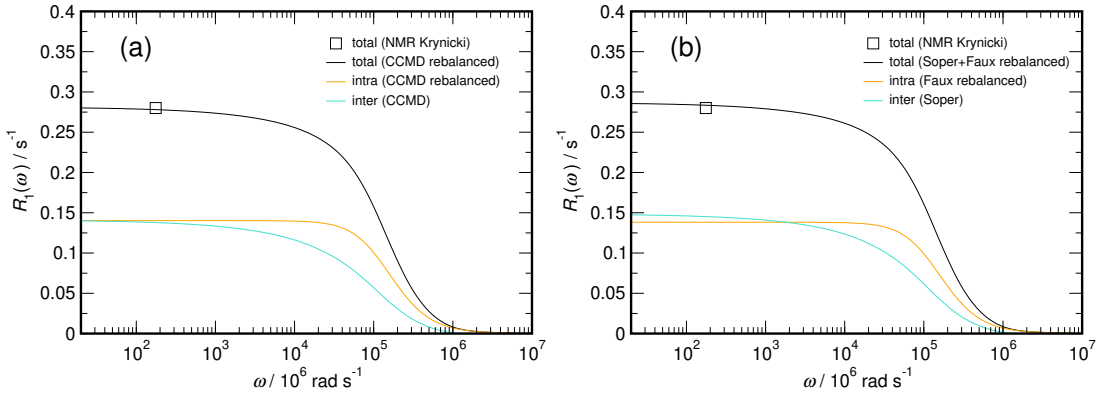


FIG. 8. Refined frequency dependent ^1H NMR relaxation rate $R_1(\omega)$ of water at 298 K at a density of 0.997 g cm^{-3} computed using the intramolecular spectral densities $J_{\text{intra}}^n(\omega)$ obtained from CCMD scaled to match the experimental balance of $D_0 \times \tau_{\text{HH}}$ a) employing the refined structural parameters from CCMD and b) employing the refined structural parameters based on the experimental data.

with

$$\Delta J_{\text{inter}}^n(\omega) \approx \int_0^{t_{\text{tr}}} \Delta G_{\text{inter}}^n(t) \cos(\omega t) dt. \quad (44)$$

Here the integration in Equation 44 is performed numerically employing the trapezoidal rule up to the time t_{tr} , where both functions $G_{\text{inter}}^{\text{n,MD}}(t)$ and $G_{\text{inter}}^{\text{n,HF}}(t)$ are deemed indistinguishable. To properly predict $J_{\text{inter}}^{\text{n,MD}}(\omega)$ for systems with $L \rightarrow \infty$, we employ the system size independent self-diffusion coefficient D_0 for computing $J_{\text{inter}}^{\text{n,HF}}(\omega)$. In addition, we use

$$\Delta J_{\text{inter}}^n(\omega) \approx \frac{\Delta \tau_{\text{G},N \rightarrow \infty}}{\Delta \tau_{\text{G},N=8192}} \cdot \Delta J_{\text{inter},N=8192}^n(\omega) \quad (45)$$

to predict the behavior of $\Delta J_{\text{inter}}^n(\omega)$ for infinite system sizes. Here $\Delta J_{\text{inter},N=8192}^n(\omega)$ is the difference function computed for a system containing 8192 water molecules, and $\Delta \tau_{\text{G},N=8192} = \Delta J_{\text{inter},N=8192}^{\text{n,MD}}(0)$ and $\Delta \tau_{\text{G},N \rightarrow \infty} = \Delta J_{\text{inter},N \rightarrow \infty}^{\text{n,MD}}(0)$ is the corresponding correlation time

predicted for an infinite system size via extrapolation. The values used here are shown in FIG. 5 as a function of system size and are given in Table I of Ref.²⁴ with $\Delta \tau_{\text{G},N \rightarrow \infty} / \Delta \tau_{\text{G},N=8192} = 1.1967$ for TIP4P/2005 water at $T = 298 \text{ K}$. The intermolecular ^1H NMR relaxation rate following Equation 1 is finally computed via

$$R_{1,\text{inter}}(\omega) = \gamma_{\text{H}}^4 \hbar^2 \cdot \frac{3}{4} \cdot \left(\frac{\mu_0}{4\pi}\right)^2 \cdot \frac{8\pi}{15} \cdot \frac{\rho_{\text{H}}}{d_{\text{HH}}^3} \times \quad (46)$$

$$\left\{ J_{\text{inter}}^{\text{n,MD}}(\omega) + 4 J_{\text{inter}}^{\text{n,MD}}(2\omega) \right\}.$$

Here ρ_{H} is representing the number density of the ^1H nuclei in liquid water.

The effect of the intermolecular water structure on the relaxation rate is captured by the DCA d_{HH} . For the case of the TIP4P/2005 model for water, we have determined this value to be $d_{\text{HH}} = 192.96 \text{ pm}$. Here we have used simulations containing 8192 water molecules to compute the H-H radial distribution functions shown in FIG. 6. To determine d_{HH} we have applied Equation 13 while the r^{-6} weighted integral over the pair dis-

tribution function was computed according to Equation 14. The obtained value for $d_{\text{HH}} = 192.96$ pm includes a long-range correction as described by Equation 14 and is found to be independent of the chosen cutoff-radius for $R_c \geq 0.9$ nm in Equation 14. We have also computed corresponding DCAs from the experimental pair distribution data according to Soper²⁹ shown in FIG. 6a, leading to $d_{\text{HH}} = 188.30$ pm, and the CCMD dataset for H₂O shown in FIG. 6b, leading to $d_{\text{HH}} = 195.68$ pm. When using the same TIP4P/2005 derived $\Delta J_{\text{inter}}^n(\omega)$ functions for all three datasets, we determine relaxation rates at $\nu_{\text{H}} = 28$ MHz of $R_{1,\text{inter}}(\nu_{\text{H}}) = 0.1405 \text{ s}^{-1}$ for the TIP4P/2005 model, $R_{1,\text{inter}}(\nu_{\text{H}}) = 0.1453 \text{ s}^{-1}$ for the experimental structure and $R_{1,\text{inter}}(\nu_{\text{H}}) = 0.1378 \text{ s}^{-1}$ for the CCMD dataset for H₂O. Note that the deviation with respect to the relaxation rate of the TIP4P/2005 model are in both cases less than 2%. Hence, the intermolecular relaxation rate $R_{1,\text{inter}}$ is found to be not very sensitive with respect to small changes of d_{HH} . The reason for this can be explained by the Hwang Freed theory which shows that the DCA d_{HH} affects both the prefactor and the correlation time $\tau_{\text{G}}^{\text{HF}} = (4/9) \cdot d_{\text{HH}}^2/D'$ such that $R_{1,\text{inter}} \propto 1/d_{\text{HH}}$. Given the insensitivity of the computed intermolecular relaxation rate with respect to structural information collected from different sources, and the fact that diffusion coefficients obtained for both TIP4P/2005 and CCMD simulations agree with the experimental value, we conclude that the computed intermolecular relaxation rates reported here can be considered a rather robust estimate.

D. Computing the Frequency-Dependent NMR Relaxation of ¹H Nuclei in Liquid Water

In FIG. 7a we have plotted the frequency-dependent inter- and intramolecular contributions to the ¹H NMR relaxation rate according to Equations 46 and 34 for the TIP4P/2005 model as discussed in Ref.²⁴. By using the information about d_{HH} and r_{HH} from CCMD simulations and experimental data we arrive at the frequency-dependent relaxation rates shown in FIG. 7b. Note that refining just the structural parameters already significantly improves the agreement with the experimental data. This effect has to be mostly attributed to the improved intramolecular H-H distance.

In FIG. 8a and 8b the rebalanced intramolecular spectral density obtained from CCMD simulations is used in addition to the modified structural parameters d_{HH} and r_{HH} obtained from CCMD simulations (FIG. 8a) and from experimental data (FIG. 8b). The data computed from CCMD simulations agree within the experimental error with the experimental relaxation rate. Moreover, our analysis suggests that both the intra- and intermolecular contribution to the relaxation rate are almost identical in magnitude.

Finally, in Table I, we report the computed relaxation rates for H₂O shown in FIG. 8a for frequencies accessi-

TABLE I. Intermolecular, intramolecular, and total dipolar ¹H NMR relaxation rates as a function of the frequency $\nu = \omega/(2\pi)$ employing refined structural parameters based on CCMD data while matching the balance of $D_0 \times \tau_{\text{HH}}$ according to the CCMD simulations of H₂O water; see text. The experimental relaxation rate was obtained to be $R_1(\nu_{\text{H}}) = (0.280 \pm 0.003) \text{ s}^{-1}$ at a frequency of $\nu_{\text{H}} = 28$ MHz.¹

$\nu_{\text{H}}/\text{MHz}$	$R_{1,\text{inter}}(\nu_{\text{H}})/\text{s}^{-1}$	$R_{1,\text{intra}}(\nu_{\text{H}})/\text{s}^{-1}$	$R_1(\nu_{\text{H}})/\text{s}^{-1}$
0	0.1410	0.1404	0.2814
28	0.1378	0.1404	0.2782
50	0.1368	0.1404	0.2772
200	0.1325	0.1404	0.2729
400	0.1289	0.1404	0.2692
800	0.1238	0.1403	0.2641
1000	0.1216	0.1402	0.2618
1200	0.1197	0.1401	0.2598

ble via state-of-the-art NMR hardware. In the discussed frequency range the intramolecular relaxation rate is almost frequency independent, even at an ¹H resonance frequency of 1.2 GHz the relaxation rate deviates by only about 0.2 per cent. Due to the long-time nature of the intermolecular dipolar correlation function following a $t^{-3/2}$ power law, the intermolecular relaxation rate shows a much stronger frequency dependence with a drop of about 15 per cent at 1.2 GHz.

V. CONCLUSIONS

We have applied a recently introduced computational framework aimed at reliably determining the frequency-dependent intermolecular NMR dipole-dipole relaxation to compute the ¹H NMR relaxation rate of liquid water at ambient conditions. We have achieved this by using information from highly accurate Coupled Cluster Molecular Dynamics (CCMD) trajectories for liquid H₂O and D₂O¹⁵, which employ a high-dimensional neural network potential generated at CCSD(T) accuracy while accounting for the effect of quantum delocalization of the nuclei by employing path integral simulations. We observe a close-to-perfect agreement with experimental ¹H NMR relaxation data if both structural and dynamical information from CCMD trajectories are taken into account, while also including a re-balancing of the rotational and translational dynamics, according to product of the self-diffusion coefficient and the reorientational correlation time of the H-H vector $D_0 \times \tau_{\text{HH}}$. The inclusion of nuclear quantum effects significantly reduces the computed intramolecular contribution to the ¹H NMR relaxation rate. In addition, our analysis suggests that the intermolecular and intramolecular contribution to the ¹H NMR relaxation rate are almost similar in magnitude, unlike to what has been predicted earlier from classical MD simulations. As a conclusion, we can state that by

employing state-of-the-art condensed matter simulation techniques, a quantitative understanding of the ^1H NMR relaxation in liquid water is within reach.

ACKNOWLEDGEMENTS

DP would like to thank David W. Sawyer for sharing his knowledge about the early history of NMR relaxation experiments on water and for his helpful comments. AS thanks the Deutsche Forschungsgemeinschaft (DFG, German Research Foundation) under Grant STR-1626/2-1 (Project 459405854) for supporting this work. RL and AMCT acknowledge the Marie 383 Skłodowska-Curie Actions Doctoral Network FC Relax 384 (HORIZON-MSCA-DN-2021, 10107275) for funding. NS, HF, and DM acknowledge funding by the DFG under Germany’s Excellence Strategy – EXC 2033 – 390677874 – RESOLV.

AUTHOR DECLARATIONS

Conflict of Interest

The authors have no conflicts to disclose.

DATA AVAILABILITY STATEMENT

The data that support the findings of this study are available from the corresponding author upon reasonable request.

- ¹K. Krynicki, “Proton spin-lattice relaxation in pure water between 0°C and 110°C,” *Physica* **32**, 167–178 (1966).
- ²E. v. Goldammer and M. D. Zeidler, “Molecular motion in aqueous mixtures with organic liquids by NMR relaxation measurements,” *Ber. Bunsenges. Phys. Chem.* **73**, 4–15 (1969).
- ³A. Abragam, *The Principles of Nuclear Magnetism* (Oxford University Press, 1961).
- ⁴J. Kowalewski, “Nuclear magnetic resonance,” (Royal Society of Chemistry, 2013) Chap. Nuclear spin relaxation in liquids and gases, pp. 230–275.
- ⁵D. Kruk, R. Meier, and A. Rössler, “Translational and rotational diffusion of glycerol by means of field cycling ^1H NMR relaxometry,” *J. Phys. Chem. B* **115**, 951–957 (2011).
- ⁶D. Kruk, A. Hermann, and E. A. Rössler, “Field-cycling NMR relaxometry of viscous liquids and polymers,” *Prog. Nucl. Magn. Reson. Spectrosc.* **63**, 33–64 (2012).
- ⁷P. Honegger, V. Overbeck, A. Strate, A. Appelhagen, M. Sappl, E. Heid, C. Schröder, R. Ludwig, and O. Steinhauser, “Understanding the nature of nuclear magnetic resonance relaxation by means of fast-field-cycling relaxometry and molecular dynamics simulations: The validity of relaxation models,” *J. Phys. Chem. Lett.* **11**, 2165–2170 (2020).
- ⁸C. A. Sholl, “Nuclear-spin relaxation by translational diffusion in liquids and solids — high-frequency and low-frequency limits,” *J. Phys. C: Solid State Phys.* **14**, 447–464 (1981).
- ⁹L.-P. Hwang and J. H. Freed, “Dynamic effects of pair correlation functions on spin relaxation by translational diffusion in liquids,” *J. Chem. Phys.* **63**, 4017–4025 (1975).
- ¹⁰V. Overbeck, B. Golub, H. Schröder, A. Appelhagen, D. Paschek, K. Neymeyr, and R. Ludwig, “Probing relaxation models by means of fast field-cycling relaxometry, NMR spectroscopy and molecular dynamics simulations: Detailed insight into the translational and rotational dynamics of a protic ionic liquid,” *J. Mol. Liq.* **319**, 114207 (2020).
- ¹¹V. Overbeck, A. Appelhagen, R. Rößler, T. Niemann, and R. Ludwig, “Rotational correlation times, diffusion coefficients and quadrupolar peaks of the protic ionic liquid ethylammonium nitrate by means of ^1H fast field cycling NMR relaxometry,” *J. Mol. Liq.* **322**, 114983 (2021).
- ¹²P. Westlund and R. Lynden-Bell, “A molecular dynamics study of the intermolecular spin-spin dipole-dipole correlation function of liquid acetonitrile,” *J. Magn. Reson.* **72**, 522–531 (1987).
- ¹³J. Schnitker and A. Geiger, “NMR-quadrupole relaxation of Xenon-131 in water. A molecular dynamics simulation study,” *Z. Phys. Chem.* **155**, 29–54 (1987).
- ¹⁴A. Philips and J. Autschbach, “Proton NMR relaxation from molecular dynamics: intramolecular and intermolecular contributions in water and acetonitrile,” *Phys. Chem. Chem. Phys.* **21**, 26621–26629 (2019).
- ¹⁵J. Daru, H. Forbert, J. Behler, and D. Marx, “Coupled Cluster Molecular Dynamics of Condensed Phase Systems Enabled by Machine Learning Potentials: Liquid Water Benchmark,” *Phys. Rev. Lett.* **129**, 226001 (2022).
- ¹⁶J. Schmidt, J. Hutter, H. Spiess, and D. Sebastiani, “Beyond isotropic tumbling models: Nuclear spin relaxation in liquids from first principles,” *ChemPhysChem* **9**, 2313–2316 (2008).
- ¹⁷A. Philips, A. Marchenko, L. C. Ducati, and J. Autschbach, “Quadrupolar N-14 NMR relaxation from force-field and ab initio molecular dynamics in different solvents,” *J. Chem. Theory Comput.* **15**, 509–519 (2019).
- ¹⁸A. Philips and J. Autschbach, “Quadrupolar NMR relaxation of aqueous I-127(-), Xe-131, and Cs-133(+): A first-principles approach from dynamics to properties,” *J. Chem. Theory Comput.* **16**, 5835–5844 (2020).
- ¹⁹I.-C. Yeh and G. Hummer, “System-size dependence of diffusion coefficients and viscosities from molecular dynamics simulations with periodic boundary conditions,” *J. Phys. Chem. B* **108**, 15873–15879 (2004).
- ²⁰O. A. Moutos, Y. Zhang, I. O. Tsimpanogiannis, I. G. Economou, and E. J. Maginn, “System-size corrections for self-diffusion coefficients calculated from molecular dynamics simulations: The case of CO₂, n-alkanes, and poly(ethylene glycol) dimethyl ethers,” *J. Chem. Phys.* **145**, 074109 (2016).
- ²¹J. Busch and D. Paschek, “OrthoBoXY: A simple way to compute true self-diffusion coefficients from MD simulations with periodic boundary conditions without prior knowledge of the viscosity,” *J. Phys. Chem. B* **127**, 7983–7987 (2023).
- ²²J. Busch and D. Paschek, “An OrthoBoXY-method for various alternative box geometries,” *Phys. Chem. Chem. Phys.* **26**, 2907–2914 (2024).
- ²³P. Honegger, M. E. Di Pietro, F. Castiglione, C. Vaccarini, A. Quant, O. Steinhauser, C. Schröder, and A. Mele, “The intermolecular NOE depends on isotope selection: Short range vs. long range behavior,” *J. Phys. Chem. Lett.* **12**, 8658–8663 (2021).
- ²⁴D. Paschek, J. Busch, E. Mock, R. Ludwig, and A. Strate, “Computing the frequency-dependent NMR relaxation of ^1H nuclei in liquid water,” *J. Phys. Chem.* **160**, 074102 (2024).
- ²⁵D. Paschek, J. Busch, E. Mock, R. Ludwig, and A. Strate, “Erratum: Computing the frequency dependent nmr relaxation of ^1H nuclei in liquid water [j. chem. phys.160, 074102 (2024).],” *J. Phys. Chem.* **161**, 139902 (2024).
- ²⁶D. Marx and J. Hutter, *Ab Initio Molecular Dynamics: Basic Theory and Advanced Methods* (Cambridge University Press, 2009).
- ²⁷J. Behler, “Four Generations of High-Dimensional Neural Network Potentials,” *Chem. Rev.* **121**, 10037–10072 (2021).
- ²⁸N. Stolte, J. Daru, H. Forbert, J. Behler, and D. Marx, “Nuclear quantum effects in liquid water are negligible for struc-

- ture but significant for dynamics,” (2024), [arXiv:2410.17675](https://arxiv.org/abs/2410.17675) [[physics.chem-ph](https://arxiv.org/abs/2410.17675)].
- 29 A. K. Soper, “The radial distribution functions of water as derived from radiation total scattering experiments: Is there anything we can say for sure?” *ISRN Phys. Chem.* **2013**, 279463 (2013).
 - 30 D. A. Faux, A. A. Rahman, and P. J. McDonald, “Water as a Lévy rotor,” *Phys. Rev. Lett.* **127**, 256001 (2021).
 - 31 M. Odelius, A. Laaksonen, M. H. Levitt, and J. Kowalewski, “Intermolecular dipole-dipole relaxation. a molecular dynamics simulation,” *J. Magn. Reson. Ser. A* **105**, 289–294 (1993).
 - 32 P. A. Egelstaff, *An Introduction to the Liquid State*, 2nd ed. (Oxford University Press, Oxford, 1992).
 - 33 J. L. F. Abascal and C. Vega, “A general purpose model for the condensed phases of water: TIP4P/2005,” *J. Chem. Phys.* **123**, 234505 (2005).
 - 34 C. Vega and J. L. F. Abascal, “Simulating water with rigid non-polarizable models: a general perspective,” *Phys. Chem. Chem. Phys.* **13**, 19633–19688 (2011).
 - 35 D. van der Spoel, E. Lindahl, B. Hess, G. Groenhof, A. E. Mark, and H. J. C. Berendsen, “GROMACS: fast, flexible, and free,” *J. Comput. Chem.* **26**, 1701–1718 (2005).
 - 36 B. Hess, C. Kutzner, D. van der Spoel, and E. Lindahl, “Gromacs 4: algorithms for highly efficient, load-balanced, and scalable molecular simulation,” *J. Chem. Theory Comput.* **4**, 435–447 (2008).
 - 37 S. Nosé, “A molecular dynamics method for simulations in the canonical ensemble,” *Mol. Phys.* **52**, 255–268 (1984).
 - 38 W. G. Hoover, “Canonical dynamics: Equilibrium phase-space distributions,” *Phys. Rev. A* **31**, 1695–1697 (1985).
 - 39 S. Habershon, D. E. Manolopoulos, T. E. Markland, and T. F. Miller III, “Ring-polymer molecular dynamics: Quantum effects in chemical dynamics from classical trajectories in an extended phase space,” *Annu. Rev. Phys. Chem.* **64**, 387–413 (2013).
 - 40 W. Wagner, J. R. Cooper, A. Dittmann, J. Kijima, H. J. Kretzschmar, A. Kruse, R. Mareš, K. Oguchi, H. Sato, I. Stöcker, O. Sifner, Y. Takaishi, I. Tanishita, J. Trübenbach, and T. Willkommen, “The IAPWS industrial formulation 1997 for the thermodynamic properties of water and steam,” *J. Eng. Gas Turbines Power* **122**, 150–180 (2000).
 - 41 S. Herrig, M. Thol, A. H. Harvey, and E. W. Lemmon, “A Reference Equation of State for Heavy Water,” *J. Phys. Chem. Ref. Data* **47**, 043102 (2018).
 - 42 Q. Yu, C. Qu, P. L. Houston, R. Conte, A. Nandi, and J. L. Bowman, “q-AQUA: A many-body CCSD(T) water potential, including four-body interactions, demonstrates the quantum nature of water from clusters to the liquid phase,” *J. Phys. Chem. Lett.* **13**, 5068–5074 (2022).
 - 43 M. S. Chen, J. Lee, H.-Z. Ye, T. C. Berkelbach, D. R. Reichman, and T. E. Markland, “Data-Efficient Machine Learning Potentials from Transfer Learning of Periodic Correlated Electronic Structure Methods: Liquid Water at AFQMC, CCSD, and CCSD(T) Accuracy,” *J. Chem. Theory Comput.* **19**, 4510–4519 (2023).
 - 44 J. Behler and M. Parrinello, “Generalized neural-network representation of high-dimensional potential-energy surfaces,” *Phys. Rev. Lett.* **98**, 146401 (2007).
 - 45 CP2K Open Source Molecular Dynamics, <https://www.cp2k.org/>.
 - 46 J. Hutter, M. Iannuzzi, F. Schiffrmann, and J. Vandevondele, “CP2K: Atomistic simulations of condensed matter systems,” *WIREs Comput. Mol. Sci.* **4**, 15–25 (2014).
 - 47 F. Briauc, C. Schran, F. Uhl, H. Forbert, and D. Marx, “Converged quantum simulations of reactive solutes in superfluid helium: The Bochum perspective,” *J. Chem. Phys.* **152**, 210901 (2020).
 - 48 C. Schran, F. Uhl, J. Behler, and D. Marx, “High-Dimensional Neural Network Potentials for Solvation: The Case of Protonated Water Clusters in Helium,” *J. Chem. Phys.* **148**, 102310 (2018).
 - 49 M. Ceriotti, M. Parrinello, T. E. Markland, and D. E. Manolopoulos, “Efficient stochastic thermostating of path integral molecular dynamics,” *J. Chem. Phys.* **133**, 124104 (2010).
 - 50 T. F. Miller and D. E. Manolopoulos, “Quantum diffusion in liquid water from ring polymer molecular dynamics,” *J. Chem. Phys.* **123**, 154504 (2005).
 - 51 D. M. Wilkins, D. E. Manolopoulos, S. Pipolo, D. Laage, and J. T. Hynes, “Nuclear Quantum Effects in Water Reorientation and Hydrogen-Bond Dynamics,” *J. Phys. Chem. Lett.* **8**, 2602–2607 (2017).
 - 52 A. Esser, H. Forbert, and D. Marx, “Tagging effects on the mid-infrared spectrum of microsolvated protonated methane,” *Chem. Sci.* **9**, 1560–1573 (2018).
 - 53 B. Dünweg and K. Kremer, “Molecular dynamics simulation of a polymer chain in solution,” *J. Chem. Phys.* **99**, 6983–6997 (1993).
 - 54 J. Busch and D. Paschek, “Computing accurate true self-diffusion coefficients and shear viscosities using the OrthoBoXY-approach,” *J. Phys. Chem. B* **128**, 1040–1052 (2024).
 - 55 M. González and J. Abascal, “The shear viscosity of rigid water models,” *J. Chem. Phys.* **132**, 096101 (2010).
 - 56 K. Krynicki, C. D. Green, and D. W. Sawyer, “Pressure and temperature dependence of self-diffusion in water,” *Faraday Discuss. Chem. Soc.* **66**, 199–208 (1978).
 - 57 M. Holz, S. R. Heil, and A. Sacco, “Temperature-dependent self-diffusion coefficients of water and six selected molecular liquids for calibration in accurate ^1H NMR PFG measurements,” *Phys. Chem. Chem. Phys.* **2**, 4740–4742 (2000).
 - 58 R. Mills, “Self-diffusion in normal and heavy water in the range 1–45°,” *J. Phys. Chem.* **77**, 685–688 (1973).
 - 59 E. A. Rössler, M. Hofmann, and N. Fatkulin, “Application of field-cycling ^1H NMR relaxometry to the study of translational and rotational dynamics in liquids and polymers,” in *New Developments in NMR*, Vol. 18, edited by E. Kimmich (Royal Society of Chemistry, 2019) Chap. 7, pp. 181–206.
 - 60 D. N. Asthagiri, W. G. Chapman, G. J. Hirasaki, and P. M. Singer, “NMR ^1H - ^1H dipole relaxation in fluids: Relaxation of individual ^1H - ^1H pairs versus relaxation of molecular modes,” *J. Phys. Chem. B* **124**, 10802–10810 (2020).
 - 61 A. V. Parambathu, P. J. Pinheiro dos Santos, W. G. Chapman, G. J. Hirasaki, D. N. Asthagiri, and P. M. Singer, “Molecular modes elucidate the nuclear magnetic resonance relaxation of viscous fluids,” *J. Phys. Chem. B* **128**, 8017–8028 (2024).
 - 62 T. Kawasaki and K. Kim, “Spurious violation of the Stokes-Einstein-Debye relation in supercooled water,” *Sci. Rep.* **9**, 8118 (2019).
 - 63 D. A. Turton and K. Wynne, “Stokes-Einstein-Debye failure in molecular orientational diffusion: Exception or rule?” *J. Phys. Chem. B* **118**, 4600–4604 (2014).
 - 64 T. Köddermann, R. Ludwig, and D. Paschek, “On the validity of Stokes-Einstein and Stokes-Einstein-Debye relations in ionic liquids and ionic-liquid mixtures,” *ChemPhysChem* **9**, 1851–1858 (2008).
 - 65 D. Laage and J. T. Hynes, “A molecular jump mechanism of water reorientation,” *Science* **311**, 832–835 (2006).
 - 66 D. Laage and J. T. Hynes, “On the molecular mechanism of water reorientation,” *J. Phys. Chem. B* **112**, 14230–14242 (2008).
 - 67 A. Gomez, Z. A. Piskulich, W. H. Thompson, and D. Laage, “Water diffusion proceeds via a hydrogen-bond jump exchange mechanism,” *J. Phys. Chem. Lett.* **13**, 460–4666 (2022).
 - 68 C. Herrero, M. Pauletti, G. Tocci, M. Iannuzzi, and L. Joly, “Connection between water’s dynamical and structural properties: Insights from ab initio simulations,” *Proc. Natl. Acad. Sci. USA* **119**, e2121641119 (2022).